Acta Polytechnica **61**(6):762–767, 2021
https://doi.org/10.14311/AP.2021.61.0762

Published by the Czech Technical University in Prague

CAVITATION WEAR OF EUROFER 97, CR18NI10TI AND 42HNM ALLOYS

Hanna Rostova[a,*], Victor Voyevodin[a,b], Ruslan Vasilenko[a], Igor Kolodiy[a], Vladimir Kovalenko[a], Vladimir Marinin[a], Valeriy Zuyok[a], Alexander Kuprin[a]

[a] *National Science Center Kharkiv Institute of Physics and Technology, Institute of Solid State Physics, Materials Science and Technologies NAS of Ukraine, 1 Akademichna Str., 61108 Kharkiv, Ukraine*

[b] *V.N. Karazin National University, Physics and Technology Faculty, Department of Reactor Materials and Physical Technologies, 4 Svobody Sq., 61022 Kharkiv, Ukraine*

[*] corresponding author: rostova@kipt.kharkov.ua

Abstract. The microstructure, hardness and cavitation wear of Eurofer 97, Cr18Ni10Ti and 42HNM have been investigated. It was revealed that the cavitation resistance of the 42HNM alloy is by an order of magnitude higher than that of the Cr18Ni10Ti steel and 16 times higher than that of the Eurofer 97 steel. Alloy 42HNM has the highest microhardness (249 kg/mm^2) of all the investigated materials, which explains its high cavitation resistance. The microhardness values of the Cr18Ni10Ti steel and the Eurofer 97 were 196.2 kg/mm^2 and 207.2 kg/mm^2, respectively. The rate of cavitation wear of the austenitic steel Cr18Ni10Ti is 2.6 times lower than that of the martensitic Eurofer 97.

Keywords: Cavitation erosion, wear, steel, hardness, structure, resistance.

1. Introduction

Realization of ambitious programs of development and construction of nuclear power plants of a new generation (GEN IV, Terra Power Wave reactor etc.) will be possible only after solutions of problems of nuclear material science are found. Promising materials for future generations of reactors, in addition to high radiation and corrosion resistance, high mechanical characteristics, should also have an increased cavitation resistance to the coolant (supercritical water or liquid metals) [1].

Among the main promising materials for future generations of reactors, the ferrite-martensitic steel Eurofer 97 and the Cr-Ni-Mo alloy 42HNM stand out.

The Eurofer 97 is a European reference material within the framework of the European Fusion Development Agreement (EFDA)–Structural Materials. In Europe, EUROFER97 has been recognized as a prospective material [2] for first walls, divertors, blanket and vessels of fast breeder reactors [3–8]. One of the main reason for its selection are the high mechanical properties at service temperatures coupled with the low or reduced activation characteristic under radiation with the result of a very low loss of mechanical properties of the Eurofer 97 steel. This material behaviour has been reported in many studies and important initiatives are still ongoing [9–11].

Nickel superalloys are selected for their usage in nuclear reactor core systems [12–17], in particular, nuclear power plants with a molten salt coolant [18–20] and Advanced Ultra Super Critical (AUSC) power plants [21, 22]. It is due to their advantage over the austenitic steels in terms of radiation and corrosion resistance (including molten salts) [12, 13] at relatively low neutron irradiation temperatures. In particular, the 42HNM alloy is considered as a candidate material for accident-resistant fuel (ATF) claddings [23].

In a moving fluid flow under certain hydrodynamic conditions, the continuity of the flow is disrupted, and cavities, caverns and bubbles are formed, which then collapse [24]. This phenomenon, occurring in the liquid flow, causes a cavitation erosion of the material [25]. Depending on the intensity of the cavitation and the time of exposure, the destruction of the metal surface can be fractions of a square millimetre, and sometimes even several square meters. The depth of the destruction of materials and products made from them is also different – up to a complete destruction. Cavitation erosion can carry away an amount of metal no lesser than corrosion; hence, the importance of studies on cavitation resistance, which will reduce metal losses and increase the durability and reliability of parts and devices, is obvious. It is known that the cavitation resistance of a material is determined by its composition and structure [26].

In this regard, in this work, we studied the cavitation wear of promising reactor materials with different crystal structures – Eurofer 97 and 42HNM. The Cr18Ni10Ti steel, widely used in nuclear power engineering, was chosen for a comparison.

2. Materials and methods of investigation

The chemical composition of the materials under study (wt. %): Eurofer 97 (C – 0.11, W – 1.4, Mn – 0.6, V – 0.25, Cr – 9.7, Ta – 0.3, Fe – balanced), 42HNM (Cr

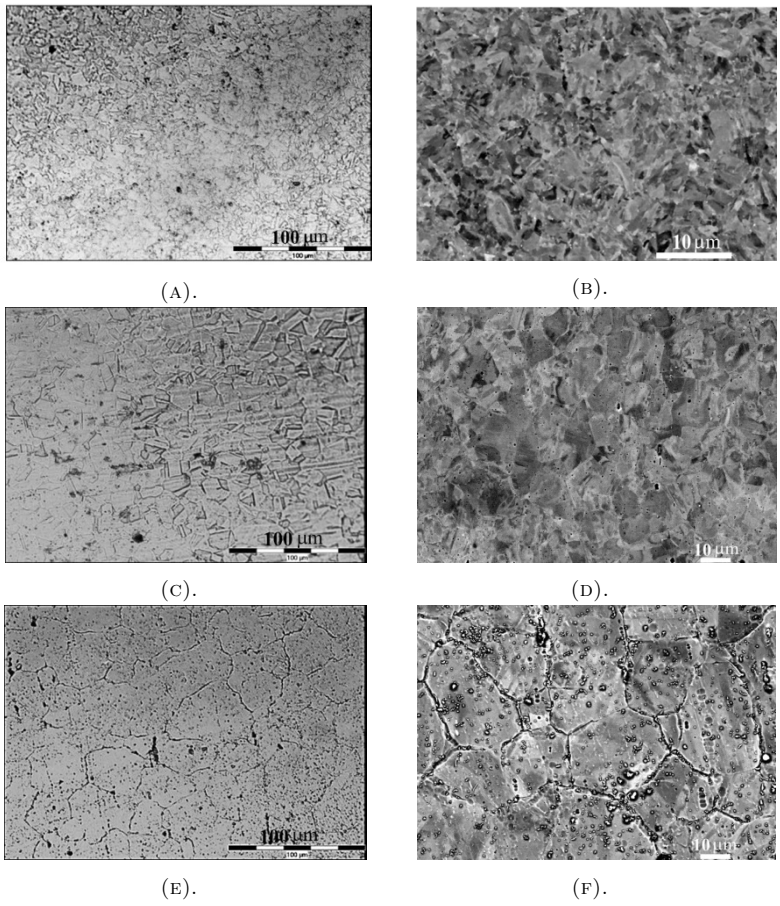

(A). (B). (C). (D). (E). (F).

FIGURE 1. Microstructure of investigated materials: Eurofer 97 – (A, B); Cr18Ni10Ti – (C, D); 42HNM – (E, F). Optical microscopy – (A, C, E) and SEM – (B, D, F) images.

– 42, Mo – 1.4, Ni – balanced) and Cr18Ni10Ti (Cr –18.7, Mn – 1.1, Ni – 10.5, Ti – 0.6, Fe – balanced). The size of the samples was $20 \times 20 \times 0.5$ mm.

The investigated materials are reactor-grade and were studied in the initial state; heat treatment modes: EUROFER97 – normalization (980 °C/27') plus tempering (760 °C/90'/air-cooled), Cr18Ni10Ti – water quenching at 1050 °C, 42HNM – austenisation at 1130 °C.

Microstructural studies were carried out on metallographic inversion microscope Olympus GX51 and on scanning electron microscope Jeol 7001-F. The specimens for metallographic studies were preliminary encapsulated into bakelite and then grinded on SiC paper (graininess from P120 to P1200) and polished on diamond suspensions with a fraction size of 1 and 0.05 μm. Etching of all samples was carried out on a Tenupol 5 setup with a reagent of 88 % ethanol + 6 % perchloric acid + 6 % glycerol at a voltage of 39 V at a room temperature.

The XRD analysis was performed on DRON-2.0 X-ray diffractometer in cobalt Co-Kα radiation, using Fe selectively-absorbing filter. The diffracted radiation was detected by a scintillation detector. Microhardness of the materials was measured on a LM 700 AT tester with a Vickers diamond indenter at a load of 2 N, with a holding time – 14 s.

Studies of the cavitation wear of the samples were carried out on a facility described in detail in the work [27, 28]. The cavitation zone was created by ultrasonic waves under the end face of the concentrator installed in a vessel with distilled water. The oscillation amplitude of the end face of the concentrator was 30 ± 2 μm at a frequency of 19.5 kHz [29]. The sample was mounted at a distance of 0.50 mm from the concentrator surface. The erosion of the samples was measured gravimetrically with an accuracy of $\pm$ 0.015 mg. The dependence of the weight loss on the time of exposure to the cavitation was measured, and from these data, kinetic curves of destruction of the samples were plotted. The average cavitation wear rate of the materials was determined in the quasilinear sections of the cavitation wear rate curves.

3. Results and discussion

The general view of the microstructure of the materials is shown in Fig. 1.

The initial structure of Eurofer 97 is tempered martensite, with prior austenite grain boundaries presence, with an average size of 6 μm (Carbon mainly in $M_{23}C_6$ and MX precipitates). The microstructure of Cr18Ni10Ti steel is austenitic with the presence of twins with an average grain size of 7.5 μm. 42HNM

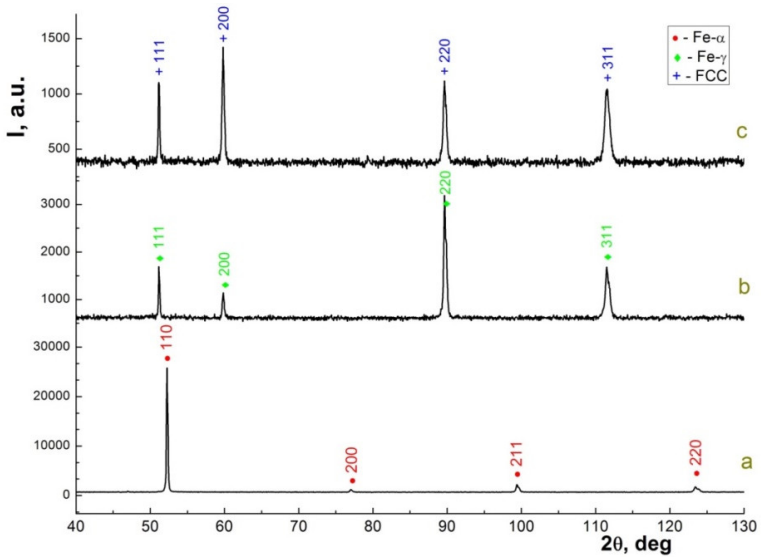

Figure 2. Diffraction patterns of the investigated samples: a) Eurofer 97; b) Cr18Ni10Ti; c) 42HNM.

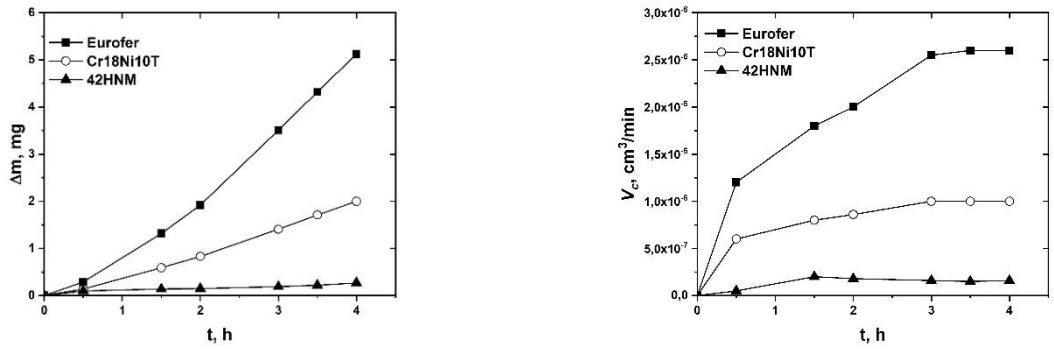

(A). (B).

Figure 3. Cavitation wear mass loss (A) and cavitation wear rate (B) for Eurofer 97, Cr18Ni10Ti and 42HNM alloys.

alloy has FCC structure and an average grain size $\sim 25\,\mu$m.

Diffraction studies have shown that all samples are single-phase, the diffraction lines in the diffractograms are narrow (Fig. 2), meaning that the samples are in a coarse-crystalline state (grain size $\geq 1\,\mu$m).

The sample Eurofer 97 consists of Fe-α ferrite/martensite with a lattice parameter $a = 2.8726$ Å. The line intensity distribution corresponds to the (110) texture. The Cr18Ni10Ti steel consists of Fe-γ austenite with a lattice parameter $a = 3.5894$ Å. The intensity distribution of the austenite lines corresponds to the (220) texture. The 42HNM alloy is also single-phase and consists of an FCC phase (solid solution based on nickel and chromium) with a lattice parameter $a = 3.5903$ Å. In the diffractogram of the sample, the intensity of the lines (200) and (220) are overestimated, which indicates a more complex texture as compared to the previous samples.

The results of the cavitation erosion experiments are shown in the form of curves of a sample mass loss depending on the test time (Fig. 3a) and curves of the rate of cavitation erosion (Fig. 3b).

From the obtained data, it can be seen that the 42HNM alloy has the highest resistance to cavitation wear of the studied materials, and the Eurofer 97 steel has the lowest one (Fig. 3a). The cavitation wear rate curves are characterized by the presence of an initial section, when the destruction is low, so-called incubation period, and a section with a maximum quasi-constant rate. The cavitation wear rate becomes constant after 3 hours of testing in the case of the investigated materials (Fig. 3b).

Mechanical properties and structural characteristics of the investigated materials are given in Table 1.

Alloy 42HNM has the highest microhardness of the investigated materials, which explains its high cavitation resistance. Despite the close values of microhardness, the rate of cavitation wear of the austenitic steel Cr18Ni10Ti is 2.6 times lower than that of the Eurofer 97 (Table 1).

Scanning electron microscopy (SEM) was used to observe the eroded surfaces of the samples after the

Alloy	**Characteristics**				
	Crystal structure	d, μm	a, Å	HV, kg/mm^2	V_c, cm^3/min
Eurofer 97	BCT	6.0	2.8726	207.2±6.0	2.6×10^{-6}
Cr18Ni10Ti	FCC	7.5	3.5894	196.2±6.1	1×10^{-6}
42HNM	FCC	25.0	3.5903	249.0±8.5	1.6×10^{-7}

TABLE 1. Crystal structure, average grain size d, lattice parameter a, microhardness HV, cavitation wear rate V_c of investigated materials.

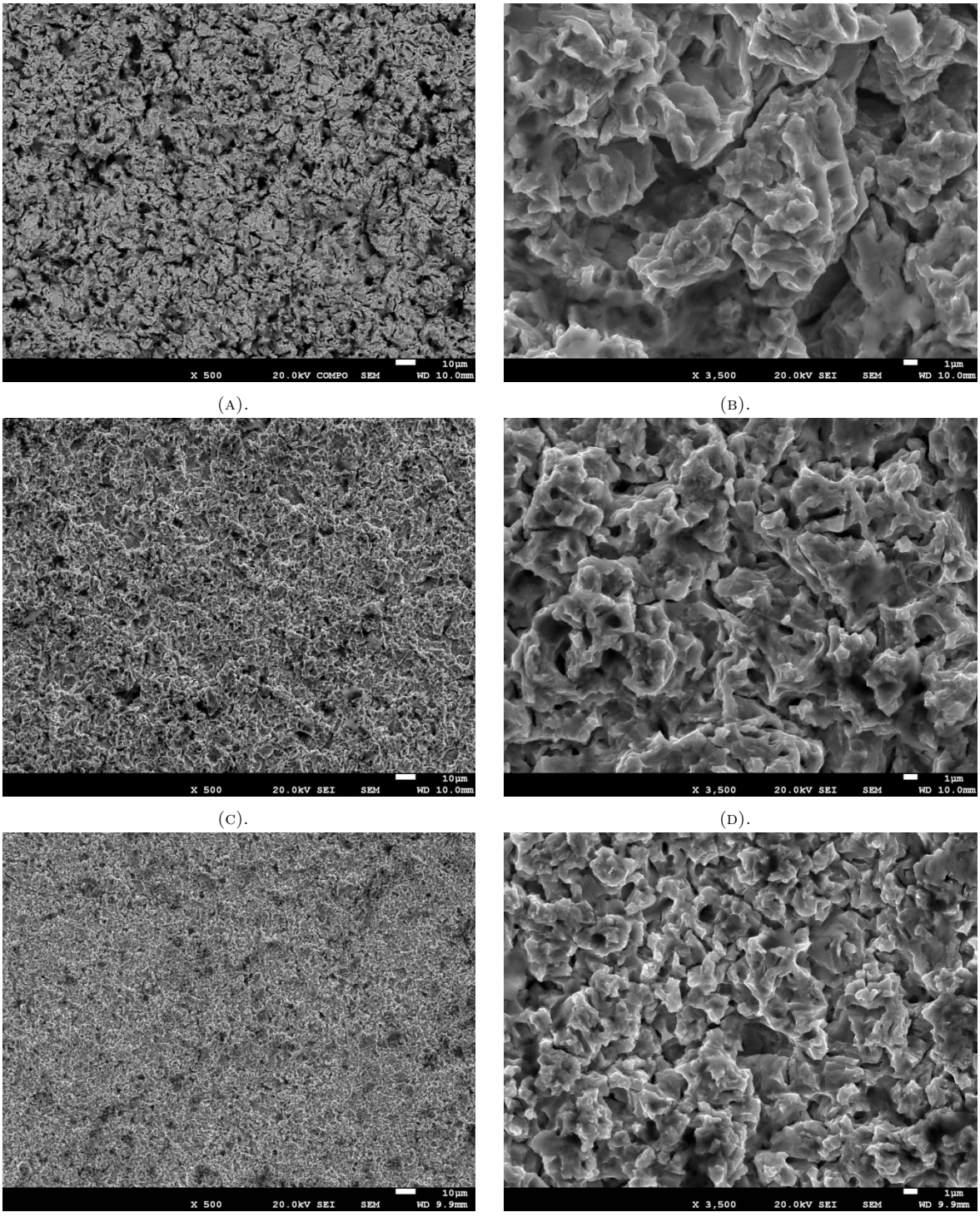

(A). (B).

(C). (D).

(E). (F).

FIGURE 4. SEM images of the eroded surfaces for the investigated materials: Eurofer 97 – (A, B); Cr18Ni10Ti – (C, D) and 42HNM – (E, F) under different magnification (A, C, E – 500; B, D, F – 3500).

4 hours of the cavitation tests. It was found that the morphologies of the eroded surfaces are different to each other in the case of Eurofer 97, Cr18Ni10Ti and 42HNM alloy (Fig. 4).

It was found that the cavitation damage for steel samples Eurofer 97 and Cr18Ni10Ti is similar in shape and is characterized by the formation of craters, pits, cracks and protruding steps on the surface of the samples. However, the difference in the degree of deformation and the size of defects is obvious for the two materials under study. The surface of Eurofer 97 steel is covered with large craters and many deep pits (Fig. 4a, 4b). The dimensions of craters and cracks are $\sim 10\,\mu$m. In the case of the Cr18Ni10Ti steel, pits and cracks were significantly smaller in size (Fig. 4c, 4d). The defect sizes are at the level of $\sim 5\,\mu$m. The comparison of the SEM images clearly indicates a significantly smoother surface of the 42HNM alloy (Fig. 4e) as compared to the steel samples. In addition, the large craters observed for Eurofer 97 and Cr18Ni10Ti were not found in the case of 42HNM (Fig. 4f). The presence of small pits and cracks ($< 5\,\mu$m) for the 42HNM alloy can be associated with its high work-hardening characteristics as well as high corrosion resistance. It is known that nickel alloys with chromium and molybdenum are highly resistant to cavitation wear [30].

Usually, the resistance to cavitation erosion of martensitic and austenitic stainless steels is higher than that of ferritic stainless steels [31]. The excellent erosion resistance of martensitic stainless steels can be attributed to the uniform strain distribution and shorter effective average free martensite laths [32]. In this case, the low cavitation resistance of Eurofer 97 steel can be caused by the presence of ferrite in the steel structure.

The use of various thermomechanical treatments can significantly improve the mechanical properties of Eurofer 97 steel [33]. However, the effect of such treatments on the cavitation resistance of this steel requires further research.

4. Conclusions

The present work investigated the cavitation resistance of materials with different crystal structures: Eurofer 97 (BCT) and Cr18Ni10Ti, 42HNM (FCC).

It was shown that the cavitation wear rate in distilled water for the 42HNM alloy is $1.6\times10^{-7}\,\mathrm{cm}^3/\mathrm{min}$, $\sim 1\times10^{-6}\,\mathrm{cm}^3/\mathrm{min}$ for Cr18Ni10Ti and $2.6\times10^{-6}\,\mathrm{cm}^3/\mathrm{min}$ for Eurofer 97.

It was found that after the cavitation tests, the morphology of eroded surfaces differs from each other for the alloy Eurofer 97, Cr18Ni10Ti and 42HNM and is in good agreement with the rate of cavitation wear. The surface of Eurofer 97 steel is covered with large craters and a large number of deep pits; for Cr18Ni10Ti steel, the size of these defects is 2 times smaller. 42HNM alloy has the smallest size of erosion defects.

Further studies are required to determine the effect of various thermomechanical treatments on the structure and cavitation resistance of the Eurofer 97 steel.

Acknowledgements

This work was prepared within the project № 6541230, implemented with the financial support of the National Academy of Science of Ukraine.

References

[1] M. Lee, Y. Kim, Y. Oh, et al. Study on the cavitation erosion behavior of hardfacing alloys for nuclear power industry. *Wear* **255**(1-6):157–161, 2003. https://doi.org/10.1016/S0043-1648(03)00144-3.

[2] M. Rieth, B. Dafferner, H. D. Rohrig, C. Wassilew. Charpy impact properties of martensitic 10.6 % Cr steel (MANET-I) before and after neutron exposure. *Fusion Engineering and Design* **29**:365–370, 1995. https://doi.org/10.1016/0920-3796(95)80043-W.

[3] K. D. Zilnyk, V. B. Oliveira, H. R. Z. Sandim, et al. Martensitic transformation in EUROFER-97 and ODS-EUROFER steels: A comparative study. *Journal of Nuclear Materials* **462**:360–367, 2015. https://doi.org/10.1016/j.jnucmat.2014.12.112.

[4] A. Möslang. IFMIF: the intense neutron source to qualify materials for fusion reactors. *Comptes Rendus Physique* **9**(3-4):457–468, 2008. https://doi.org/10.1016/j.crhy.2007.10.018.

[5] S. J. Zinkle, G. S. Was. Materials challenges in nuclear energy. *Acta Materialia* **61**(3):735–758, 2013. https://doi.org/10.1016/j.actamat.2012.11.004.

[6] Y. Guerin, G. S. Was, S. J. Zinkle. Materials challenges for advanced nuclear energy systems. *MRS Bulettin* **34**(1):10–19, 2009. https://doi.org/10.1017/S0883769400100028.

[7] G. H. Marcus. Innovative nuclear energy systems and the future of nuclear power. *Progress in Nuclear Energy* **50**(2-6):92–96, 2008. https://doi.org/10.1016/j.pnucene.2007.10.009.

[8] K. Ehrlich, J. Konys, L. Heikinheimo. Materials for high performance light water reactors. *Journal of Nuclear Materials* **327**(2-3):140–147, 2004. https://doi.org/10.1016/j.jnucmat.2004.01.020.

[9] R. L. Klueh, D. R. Harries. *High-Chromium Ferritic and Martensitic Steels for Nuclear Applications.* West Conshohocken, PA: ASTM International, 2001. https://doi.org/10.1520/MONO3-EB.

[10] L. Tan, D. T. Hoelzer, J. T. Busby, et al. Microstructure control for high strength 9Cr ferritic-martensitic steels. *Journal of Nuclear Materials* **422**(1-3):45–50, 2012. https://doi.org/10.1016/j.jnucmat.2011.12.011.

[11] L. Tan, X. Ren, T. R. Allen. Corrosion behaviour of 9-12 % Cr ferritic-martensitic steels in supercritical water. *Corrosion Science* **52**(4):1520–1528, 2010. https://doi.org/10.1016/j.corsci.2009.12.032.

[12] M. I. Solonin, A. B. Alekseev, S. A. Averin, et al. Cr-Ni alloys for fusion reactors. *Journal of Nuclear Materials* **258-263**(2):1762–1766, 1998. https://doi.org/10.1016/S0022-3115(98)00406-1.

[13] A. V. Vatulin, V. P. Kondrat'ev, V. N. Rechitskii, M. I. Solonin. Corrosion and radiation resistance of "Bochvaloy" nickel-chromium alloy. *Metal Science and Heat Treatment* **46**(11-12):469–473, 2004. https://doi.org/10.1007/s11041-005-0004-8.

[14] A. F. Rowcliffe, L. K. Mansur, D. T. Hoelzer, R. K. Nanstad. Perspectives on radiation effects in nickel-base alloys for applications in advanced reactors. *Journal of Nuclear Materials* **392**(2):341–352, 2009. https://doi.org/10.1016/j.jnucmat.2009.03.023.

[15] M. Stopher. The effects of neutron radiation on nickel-based alloys. *Materials Science and Technology* **33**(5):518–536, 2017. https://doi.org/10.1080/02670836.2016.1187334.

[16] M. I. Solonin, A. B. Alekseev, Y. I. Kazennov, et al. XHM-1 alloy as a promising structural material for water-cooled fusion reactor components. *Journal of Nuclear Materials* **233-237**(1):586–591, 1996. https://doi.org/10.1016/S0022-3115(96)00297-8.

[17] M. I. Solonin. Radiation-resistant alloys of the nickel-chromium system. *Metal Science and Heat Treatment* **47**(7-8):328–332, 2005. https://doi.org/10.1007/s11041-005-0074-7.

[18] M. de los Reyes, L. Edwards, M. A. Kirk, et al. Microstructural evolution of an ion irradiated Ni-Mo-Cr-Fe alloy at elevated temperatures. *Materials Transactions* **55**(3):428–433, 2014. https://doi.org/10.2320/matertrans.MD201311.

[19] C. Le Brun. Molten salts and nuclear energy production. *Journal of Nuclear Materials* **360**(1):1–5, 2007. https://doi.org/10.1016/j.jnucmat.2006.08.017.

[20] S. Delpech, C. Cabet, C. Slim, G. S. Picard. Molten fluorides for nuclear applications. *MaterialsToday* **13**(12):34–41, 2010. https://doi.org/10.1016/S1369-7021(10)70222-4.

[21] A. H. V. Pavan, R. L. Narayan, M. Swamy, et al. Stress rupture embrittlement in cast Ni-based superalloy 625. *Materials Science and Engineering: A* **793**(139811), 2020. Article number 139811, https://doi.org/10.1016/j.msea.2020.139811.

[22] A. H. V. Pavan, R. L. Narayan, K. Singh, U. Ramamurty. Effect of ageing on microstructure, mechanical properties and creep behavior of alloy 740H. *Metallurgical and Materials Transactions A* **51**:5169–5179, 2020. https://doi.org/10.1007/s11661-020-05951-6.

[23] B. Gurovich, A. Frolov, D. Maltsev, et al. Phase transformations in irradiated 42CrNiMo alloy after annealing at elevated temperatures, and also after rapid annealing, simulating the maximum design basis accident. In *XI Conference on reactor materials science*, pp. 30–33. AO GNTs NIIAR, Dimitrovgrad, 2019.

[24] B. Sreedhar, S. Albert, A. Pandit. Cavitation damage: Theory and measurements – a review. *Wear* **372-373**:177–196, 2017. https://doi.org/10.1016/j.wear.2016.12.009.

[25] R. H. Richman, W. P. McNaughton. A metallurgical approach to improved cavitation-erosion resistance. *Journal of Materials Engineering and Performance* **6**(5):633–641, 1997. https://doi.org/10.1007/s11665-997-0057-5.

[26] D. E. Zakrzewska, A. K. Krella. Cavitation erosion resistance influence of material properties. *Advances in Materials Science* **19**(4):18–34, 2019. https://doi.org/10.2478/adms-2019-0019.

[27] V. I. Kovalenko, V. G. Marinin. Research of fracture of doped titanium alloys under cavitation (in Russian). *Eastern-European Journal of Enterprise Technologies* **6**(11):4–8, 2015. https://doi.org/10.15587/1729-4061.2015.54118.

[28] V. G. Marinin, V. I. Kovalenko, N. S. Lomino, et al. Cavitation erosion of Ti coatings produced by the vacuum arc method. In *Proceedings ISDEIV. 19th International Symposium on Discharges and Electrical Insulation in Vacuum (Cat. No.00CH37041)*, vol. 2, pp. 567–570. IEEE, Xi'an, China, 2000. https://doi.org/10.1109/DEIV.2000.879052.

[29] ASTM G32-16, standard test method for cavitation erosion using vibratory apparatus, 2016. https://doi.org/10.1520/G0032-16.

[30] H. G. Feller, Y. Kharrazi. Cavitation erosion of metals and alloys. *Wear* **93**(3):249–260, 1984. https://doi.org/10.1016/0043-1648(84)90199-6.

[31] S. Hattori, R. Ishikura. Revision of cavitation erosion database and analysis of stainless steel data. *Wear* **268**(1-2):109–116, 2010. https://doi.org/10.1016/j.wear.2009.07.005.

[32] W. Liu, Y. G. Zheng, C. S. Liu, et al. Cavitation erosion behavior of Cr-Mn-N stainless steels in comparison with 0Cr13Ni5Mo stainless steel. *Wear* **254**(7-8):713–722, 2003. https://doi.org/10.1016/S0043-1648(03)00128-5.

[33] J. Hoffmann, M. Rieth, L. Commin, et al. Improvement of reduced activation 9 %Cr steels by ausforming. *Nuclear Materials and Energy* **6**:12–17, 2016. https://doi.org/10.1016/j.nme.2015.12.001.